Electronic Supplementary Material (ESI) for Catalysis Science & Technology.
This journal is © The Royal Society of Chemistry 2014

Catal. Sci. Technol. Electronic supplementary information (ESI)

Catalysis
Science &
Technology

PAPER

View Article Online
View Journal | View Issue

Oxidation of hydrocarbons with H_2O_2/O_2 catalyzed by osmium complexes containing *p*-cymene ligands in acetonitrile

Mikhail M. Vinogradov,[a,b,] Yuriy N. Kozlov,[c] Dmytro S. Nesterov, [b]
Lidia S. Shul'pina,[a] Armando J. L. Pombeiro,[c] and Georgiy B. Shul'pin *[,c]

[a] *Nesmeyanov Institute of Organoelement Compounds, Russian Academy of Sciences, Ulitsa Vavilova, dom 28, Moscow 119991, Russia*
[b] *Centro de Química Estrutural, Complexo I, Instituto Superior Técnico, Univercidade de Lisboa, Av. Rovisco Pais, 1049-001 Lisbon, Portugal*
[c] *Semenov Institute of Chemical Physics, Russian Academy of Science, Ulitsa Kosygina, dom 4, 119991 Moscow, Russia*

* Corresponding author. Tel.: +7 495 9397317; fax: +7499 1376130; +7495 6512191;

E-mail addresses: Shulpin@chph.ras.ru and gbsh@mail.ru (G. B. Shul'pin)

Supplementary information (ESI)

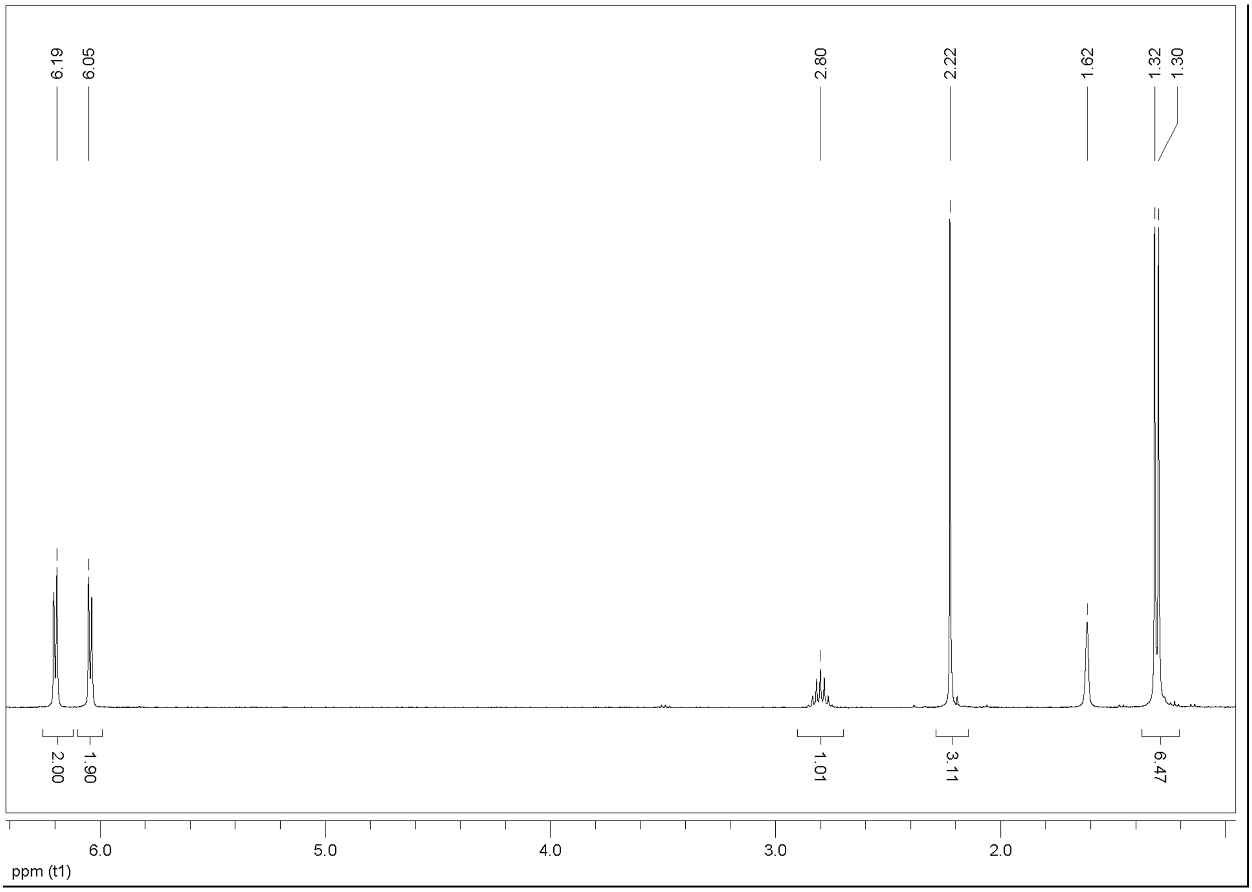

Figure S1. ^{1}H NMR spectrum of complex **1** in $CDCl_3$.

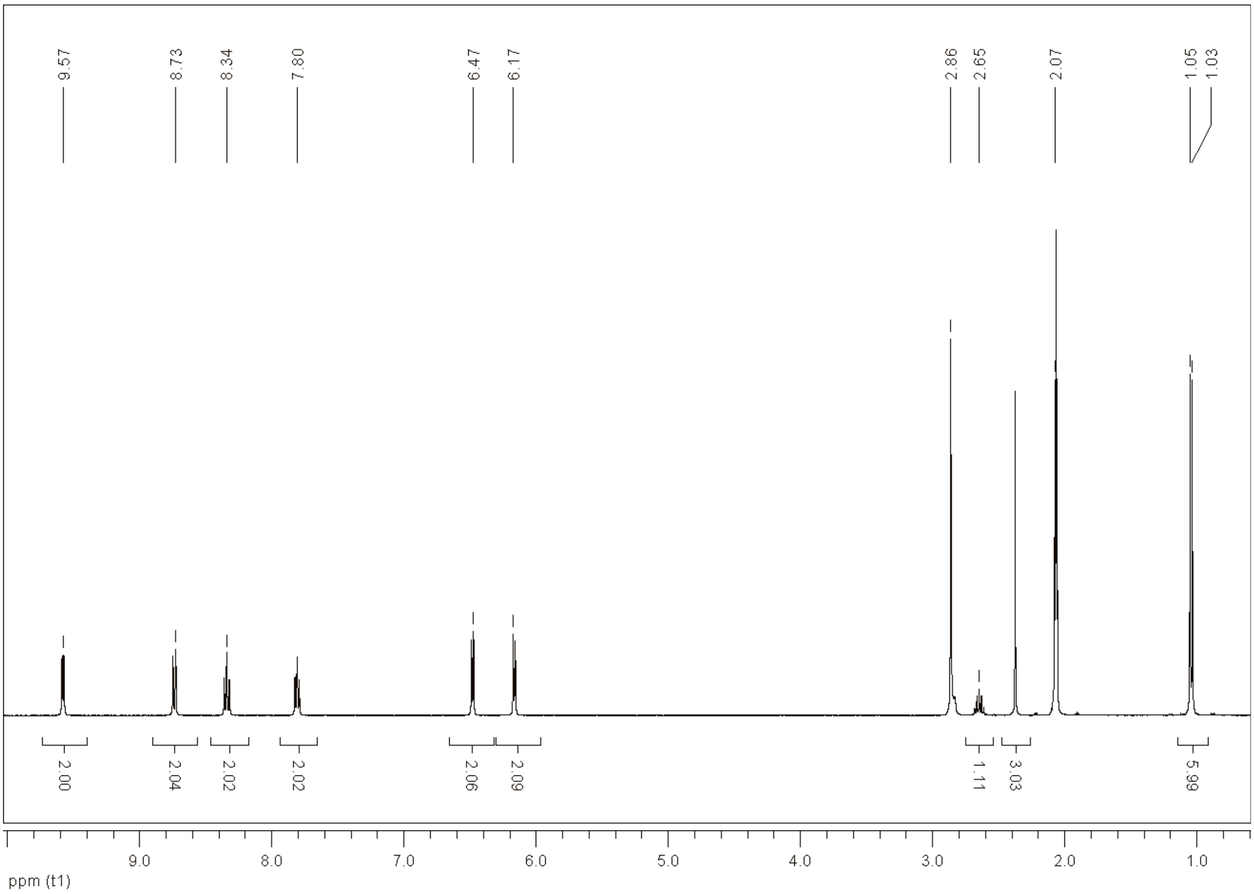

Figure S2. ^{1}H NMR spectrum of complex **2** in acetone-d_6.

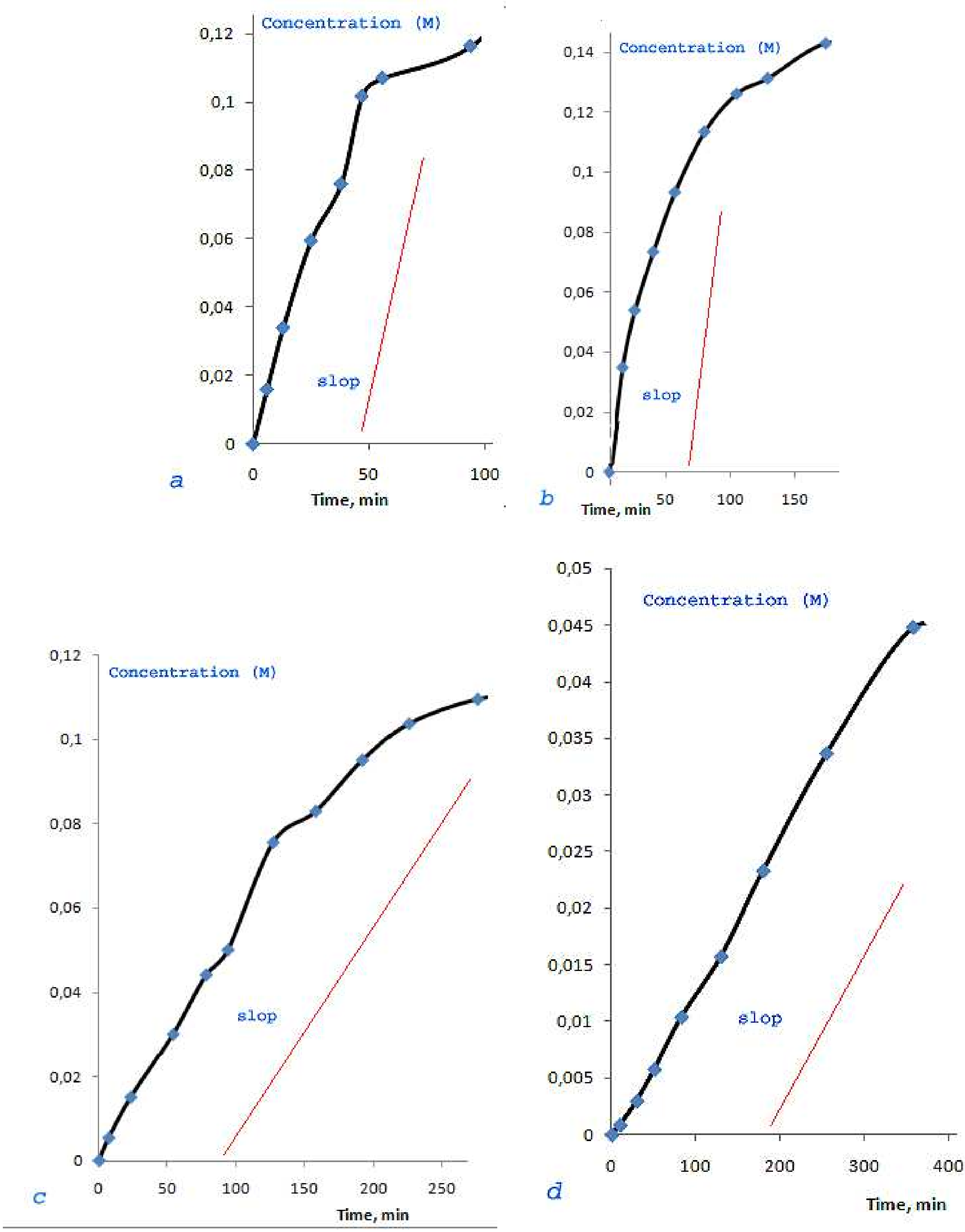

Figure S3. Accumulation of a sum of oxygenates (predominantly cyclohexyl hydroperoxide) with time in the cyclohexane oxidation with H_2O_2 catalyzed by complex **1** in acetonitrile at its different concentrations: 1×10^{-4} (graph *a*), 5×10^{-5} (graph *b*), 1×10^{-5} (graph *c*) and 1×10^{-6} M (graph *d*). The dependence is presented in Figure 3. Conditions: [py] = 0.05 M, $[\text{cyclohexane}]_0 = 0.46$ M, $[H_2O_2]_0 = 2.2$ M, $[H_2O]_{\text{total}} = 4.15$ M, 60 °C. The concentrations were measured as a sum cyclohexanol+cyclohexanone after reduction of the reaction sample with PPh_3.

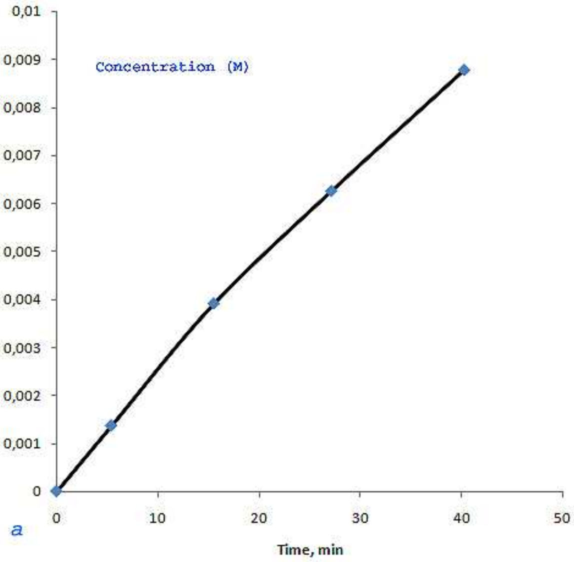
Concentration (M)
0,01
0,009
0,008
0,007
0,006
0,005
0,004
0,003
0,002
0,001
0
a
0
10
20
30
40
50
Time, min

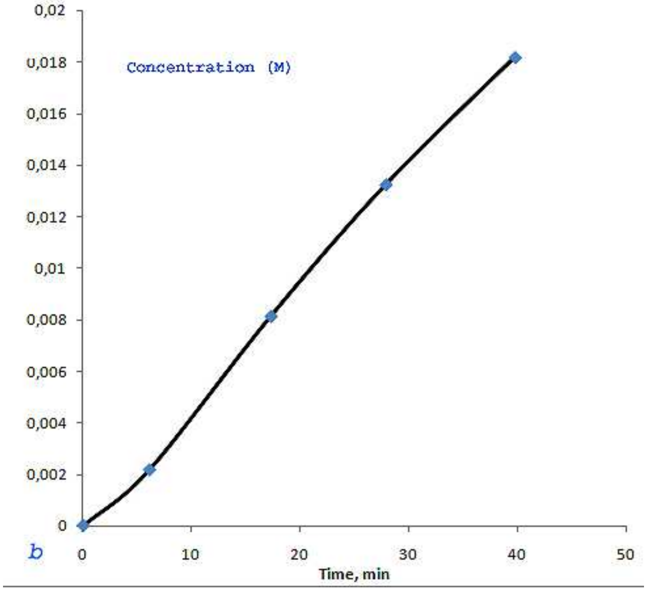
Concentration (M)
0,02
0,018
0,016
0,014
0,012
0,01
0,008
0,006
0,004
0,002
0
b
0
10
20
30
40
50
Time, min

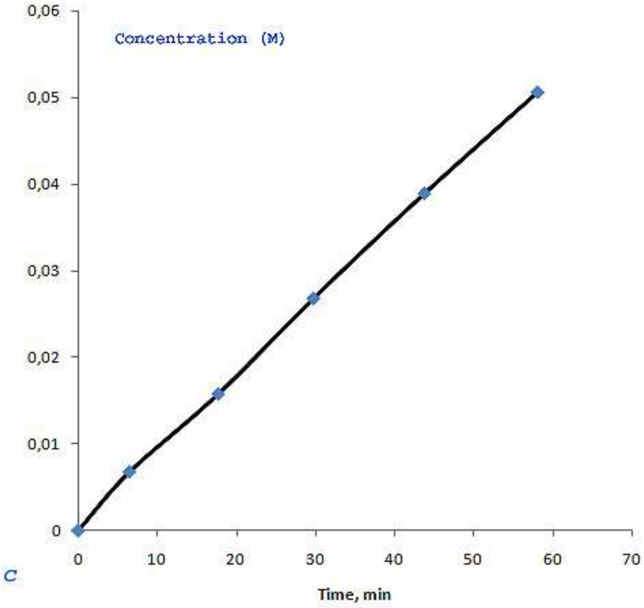
0,06
0,05
0,04
0,03
0,02
0,01
0
Concentration (M)
0
10
20
30
40
50
60
70
c
Time, min

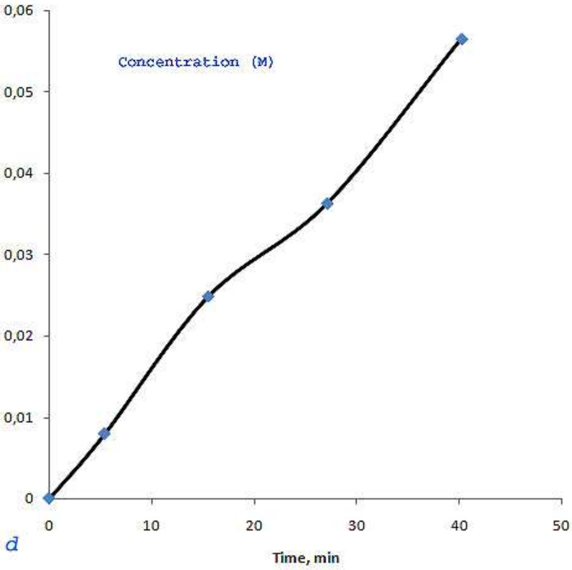
0,06
0,05
0,04
0,03
0,02
0,01
0
Concentration (M)
0
10
20
30
40
50
d
Time, min

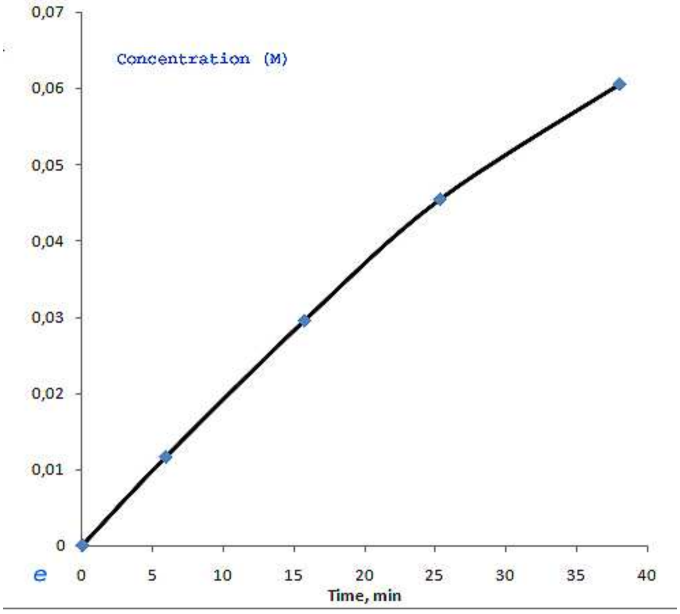

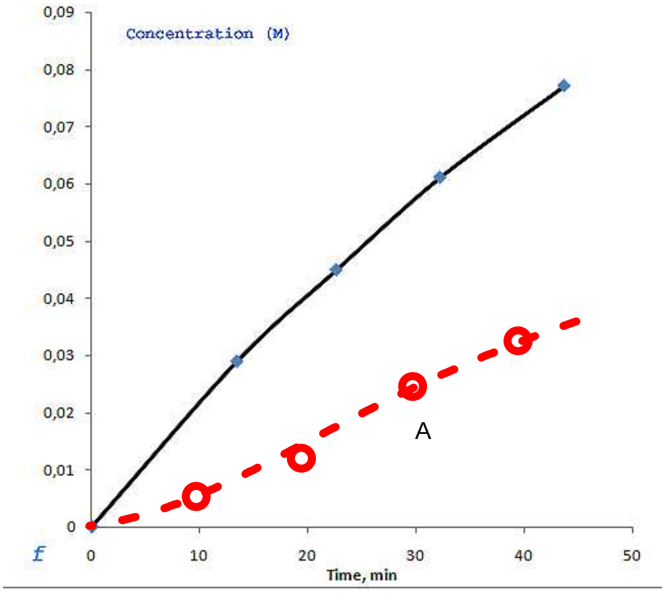

Figure S4. Accumulation of a sum of oxygenates with time in the cyclohexane oxidation with H_2O_2 catalyzed by complex **1** in acetonitrile at different concentrations of added pyridine: 0.01 (graph *a*), 0.025 (graph *b*), 0.05 (graph *c*), 0.10 (graph *d*), 0.20 (graph *e*) and 0.03 (graph *f*) M. The dependence is presented in Figure 4. Conditions: $[\mathbf{1}]_0 = 5 \times 10^{-5}$ M, $[\text{cyclohexane}]_0 = 0.46$ M, $[H_2O_2]_0 = 1.1$ M, $[H_2O]_{\text{total}} = 2.1$ M, 60 °C. The concentrations were measured as a sum cyclohexanol+cyclohexanone after reduction of the reaction sample with PPh_3. The experiment carried out under the stream of argon instead of air atmosphere is shown by dotted curve A in graph *f*.

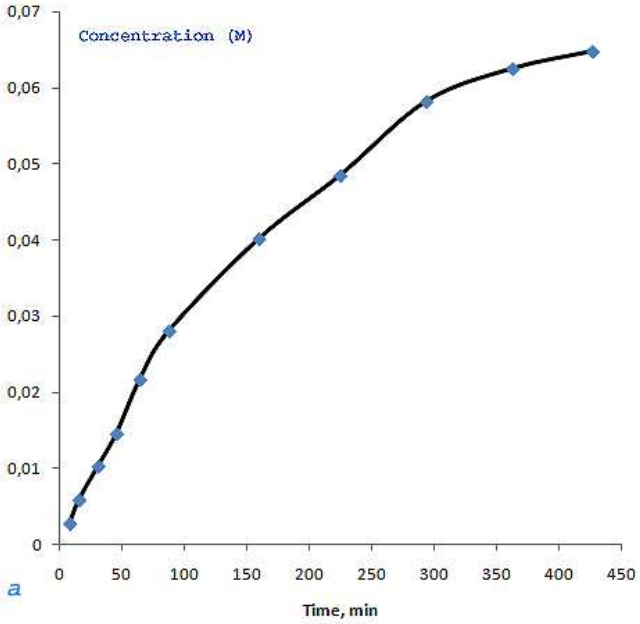
Concentration (M)
0,07
0,06
0,05
0,04
0,03
0,02
0,01
0
0
50
100
150
200
250
300
350
400
450
Time, min

a

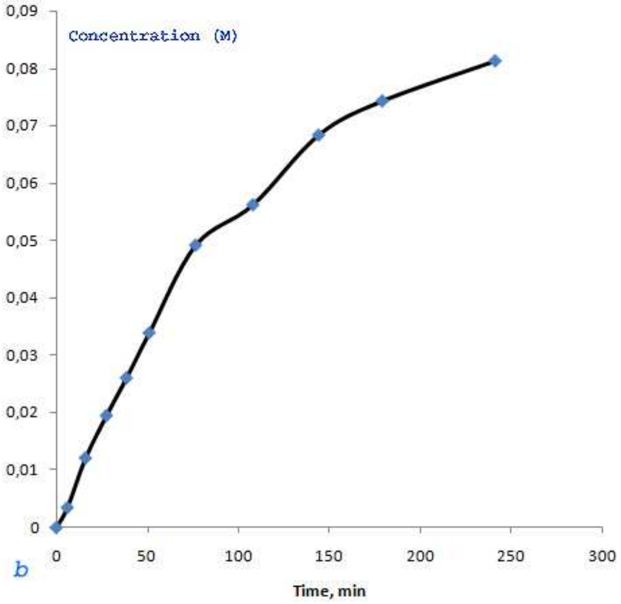
Concentration (M)
0,09
0,08
0,07
0,06
0,05
0,04
0,03
0,02
0,01
0
0
50
100
150
200
250
300
Time, min

b

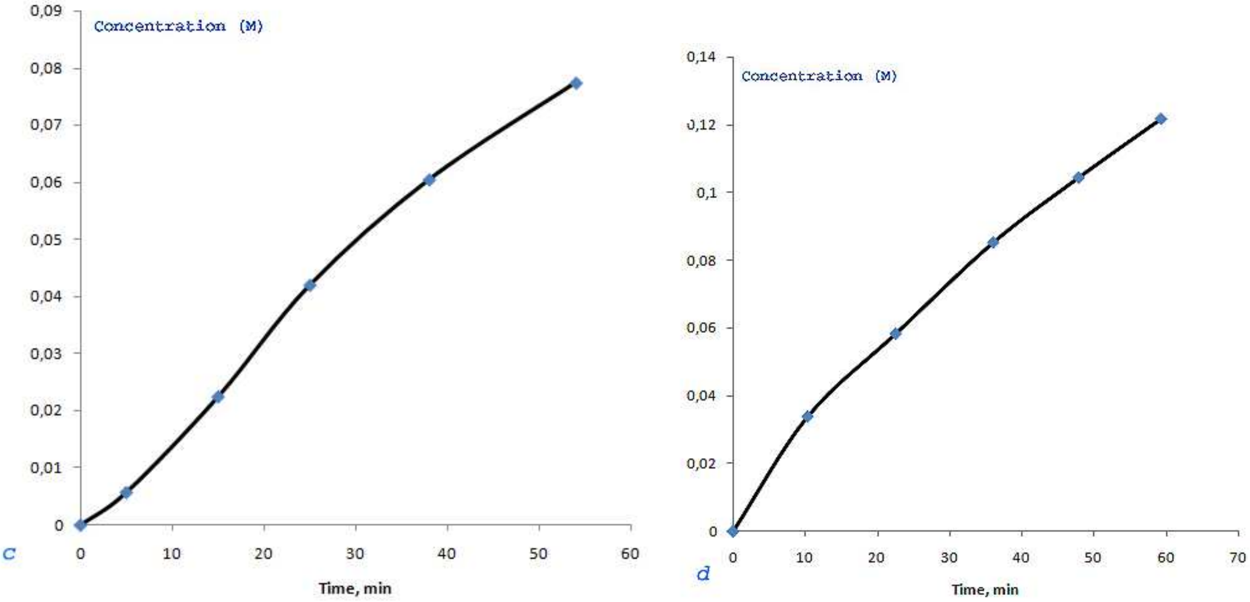

Figure S5. Accumulation of a sum of oxygenates with time in the cyclohexane oxidation with H_2O_2 catalyzed by complex **1** in acetonitrile at different initial concentrations of H_2O_2: 0.55 (graph *a*), 1.10 (graph *b*), 2.20 (graph *c*) and 3.10 (graph *d*) M. The dependence is presented in Figure 5. Conditions: $[\mathbf{1}]_0 = 5 \times 10^{-5}$ M, $[\text{cyclohexane}]_0 = 0.46$ M, $[H_2O]_{\text{total}} = \textit{const} = 5.9$ M, 60 °C. The concentrations were measured as a sum cyclohexanol+cyclohexanone after reduction of the reaction sample with PPh_3.

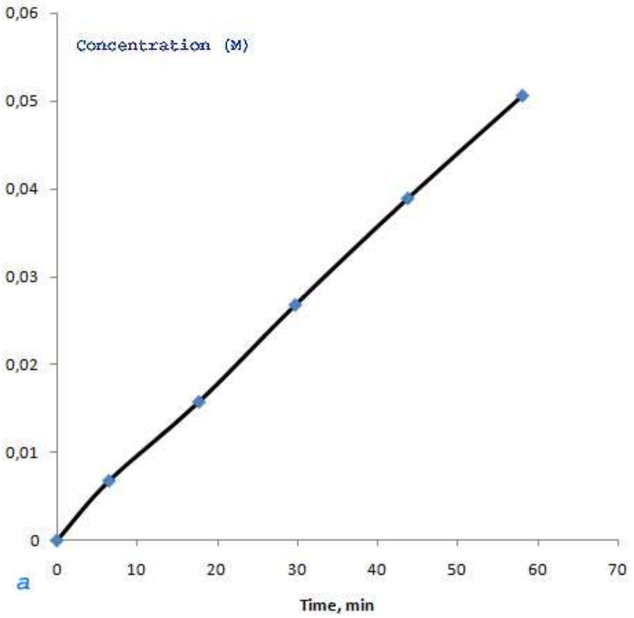
Concentration (M)
0,06
0,05
0,04
0,03
0,02
0,01
0
0
10
20
30
40
50
60
70
Time, min
a

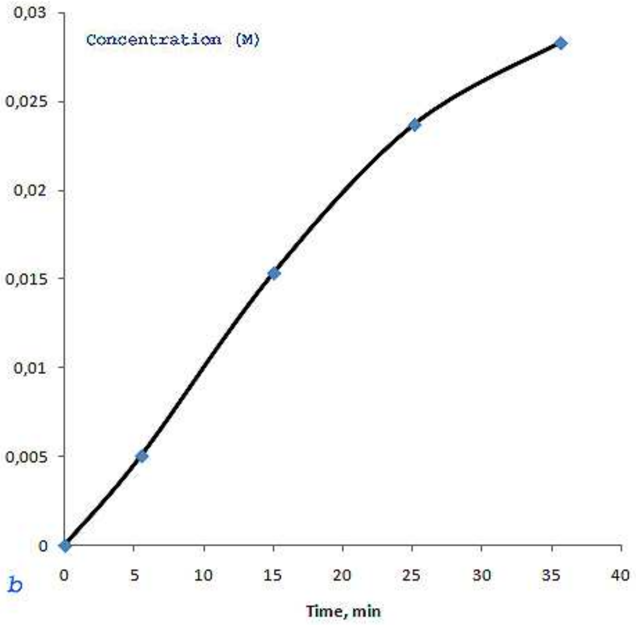
Concentration (M)
0,03
0,025
0,02
0,015
0,01
0,005
0
0
5
10
15
20
25
30
35
40
Time, min
b

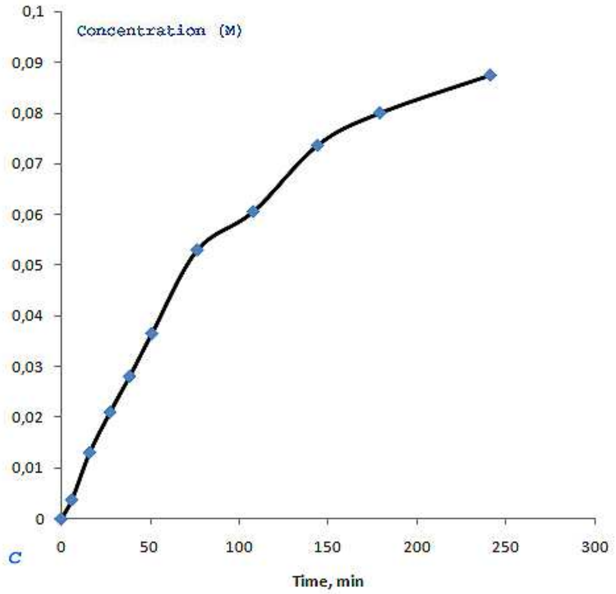

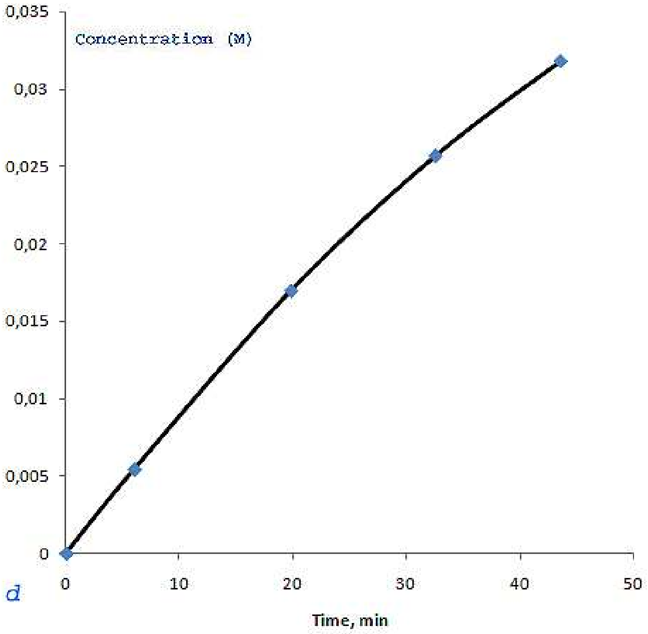

Figure S6. Accumulation of a sum of oxygenates with time in the cyclohexane oxidation with H_2O_2 catalyzed by complex **1** in acetonitrile at different totals of water: 2.1 (graph *a*), 4.0 (graph *b*), 5.9 (graph *c*) and 7.7 (graph *d*) M. The dependence is presented in Figure 6. Conditions: $[\mathbf{1}]_0 = 5 \times 10^{-5}$ M, [py] = 0.05 M, $[H_2O_2]_0 = 1.1$ M, $[\text{cyclohexane}]_0 = 0.46$ M, 60 °C. The concentrations were measured as a sum cyclohexanol+cyclohexanone after reduction of the reaction sample with PPh_3.

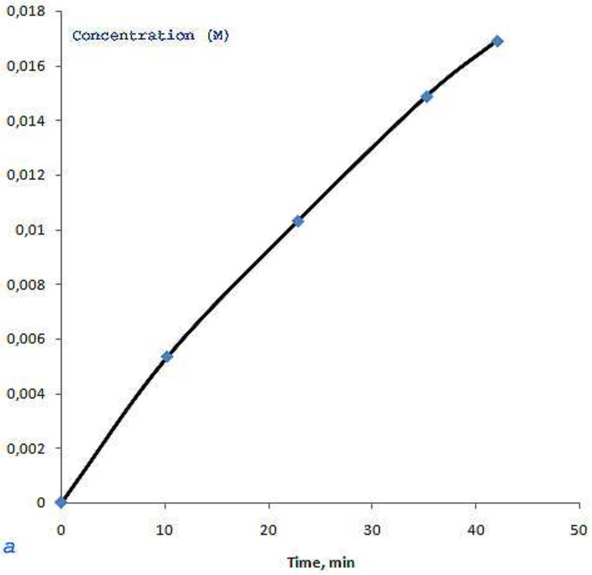
Concentration (M)
0,018
0,016
0,014
0,012
0,01
0,008
0,006
0,004
0,002
0
0
10
20
30
40
50
Time, min

a

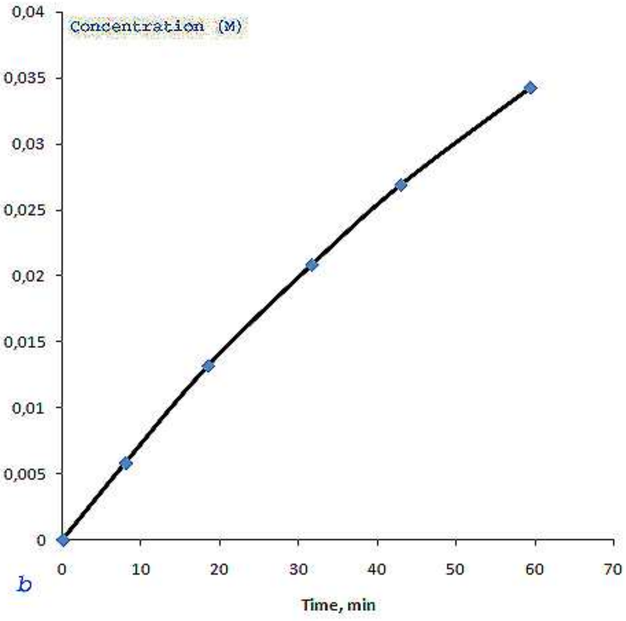
Concentration (M)
0,04
0,035
0,03
0,025
0,02
0,015
0,01
0,005
0
0
10
20
30
40
50
60
70
Time, min

b

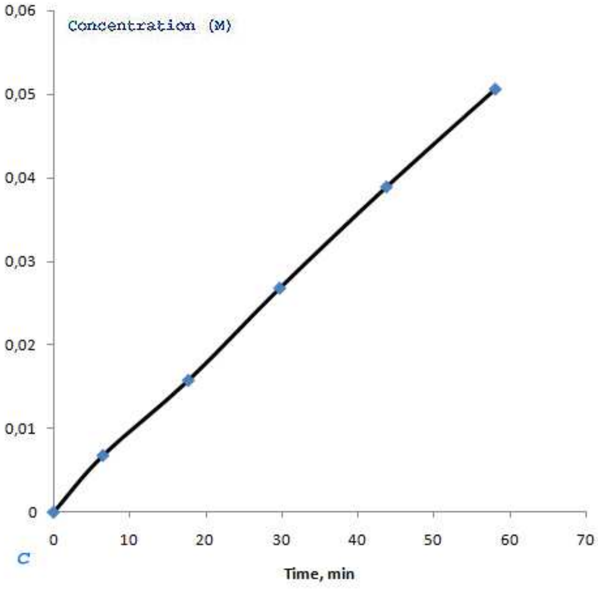
Concentration (M)
0,06
0,05
0,04
0,03
0,02
0,01
0
0
10
20
30
40
50
60
70
Time, min

c

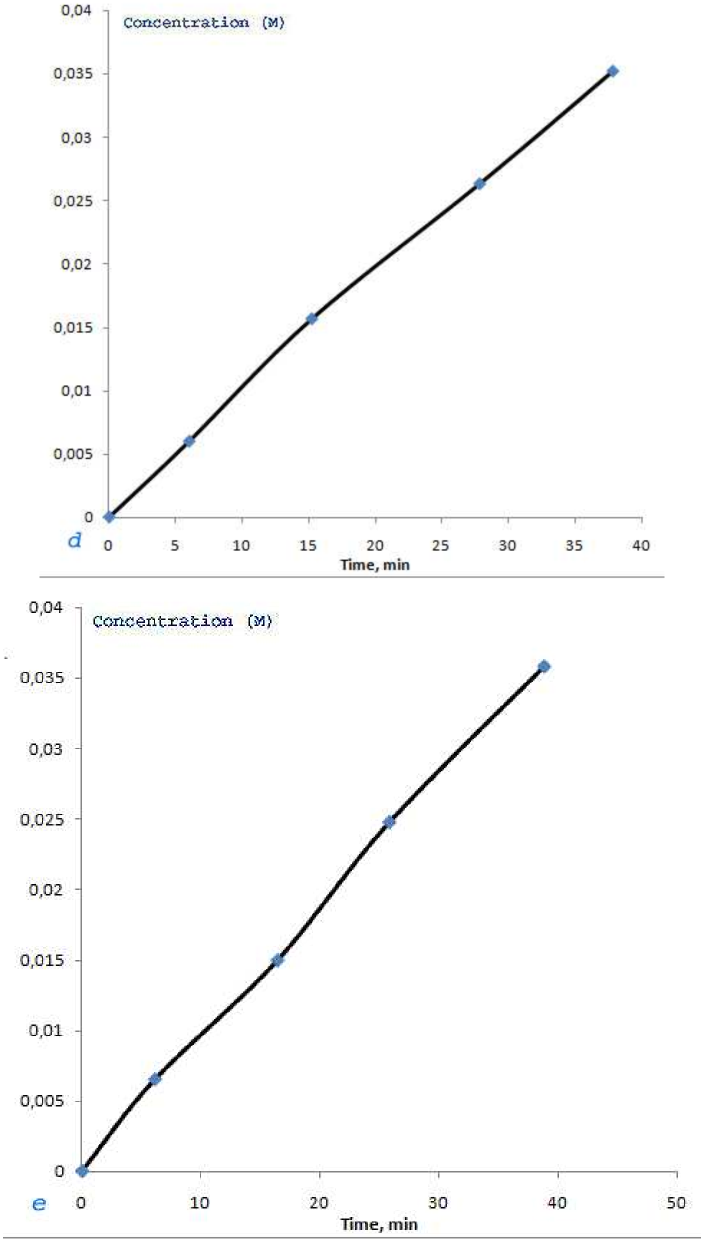

Figure S7. Accumulation of a sum of oxygenates with time in the cyclohexane oxidation with H_2O_2 catalyzed by complex **1** in acetonitrile at different initial concentrations of cyclohexane: 0.12 (graph *a*), 0.23 (graph *b*), 0.46 (graph *c*), 0.70 (graph *d*) and 0.92 M (graph *e*). The dependence is presented in Figure 6. Conditions: $[\mathbf{1}]_0 = 5 \times 10^{-5}$ M, [py] = 0.05 M, $[H_2O_2]_0 = 1.1$ M, $[H_2O]_{total} = 2.1$ M, 60 °C. The concentrations were measured as a sum cyclohexanol+cyclohexanone after reduction of the reaction sample with PPh_3.

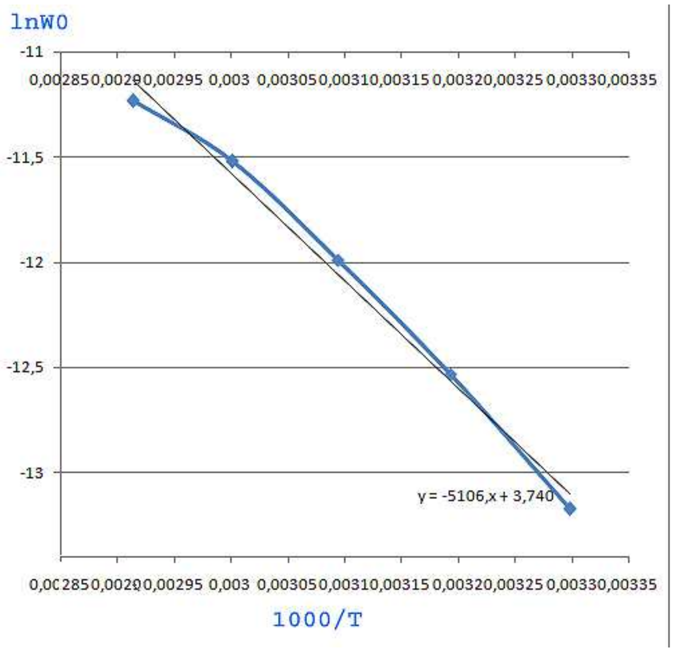

Figure S8. The Arrhenius plot for the cycohexane hydroperoxidation with H_2O_2 catalyzed by complex **1** and pyridine. Conditions: $[\mathbf{1}]_0 = 2.5 \times 10^{-5}$ M, [py] = 0.05 M, $[H_2O_2]_0 = 1.1$ M, $[H_2O]_{total} = 2.1$ M, $[\text{cyclohexane}]_0 = 0.46$ M. This dependence corresponds to the effective activation energy $E_a = 10 \pm 2$ kcal mol^{-1}. The original kinetic curves at different temperatures are presented in Figure S9.

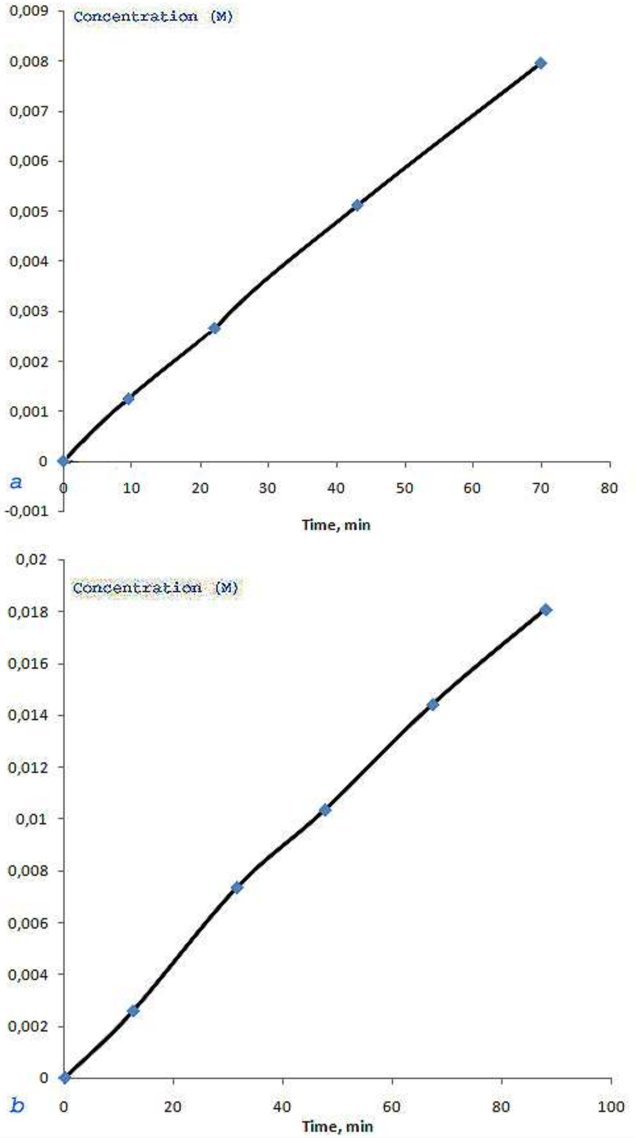
Concentration (M)
0,009
0,008
0,007
0,006
0,005
0,004
0,003
0,002
0,001
0
-0,001
a
0
10
20
30
40
50
60
70
80
Time, min
Concentration (M)
0,02
0,018
0,016
0,014
0,012
0,01
0,008
0,006
0,004
0,002
0
b
0
20
40
60
80
100
Time, min

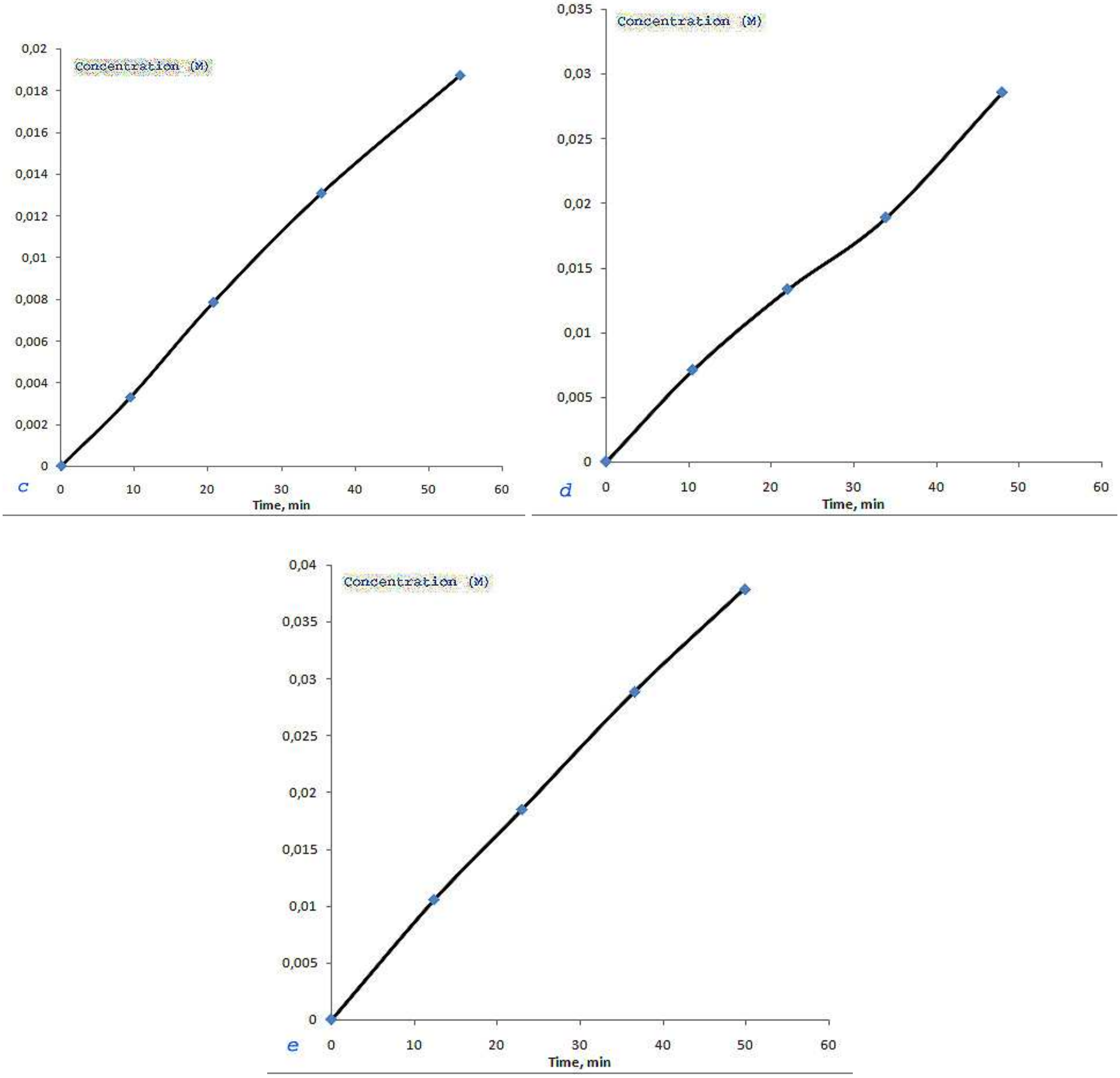

Figure S9. Accumulation of a sum of oxygenates with time in the cyclohexane oxidation with H_2O_2 catalyzed by complex **1** in acetonitrile at different temperatures: 30 (graph *a*), 40 (graph *b*), 50 (graph *c*), 60 (graph *d*) and 70 °C (graph *e*). The dependence is presented in Figure S8. Conditions: $[\mathbf{1}]_0 = 2.5 \times 10^{-5}$ M, [py] = 0.05 M, $[H_2O_2]_0 = 1.1$ M, $[H_2O]_{total} = 2.1$ M, $[\text{cyclohexane}]_0 = 0.46$ M.

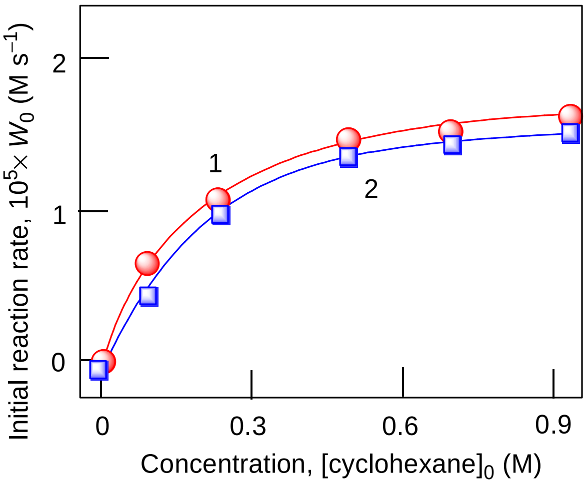

Figure S10. Dependence of initial rate W_0 of the cyclohexane oxidation with H_2O_2 catalyzed by complex **1** on initial concentration of cyclohexane in the absence (curve *1*) and in the presence of benzene (0.2 M; curve *2*). Conditions: $[\mathbf{1}]_0 = 5 \times 10^{-5}$ M, [py] = 0.05 M, $[H_2O_2]_0 = 1.1$ M, $[H_2O]_{total} = 2.1$ M, 60 °C.

Table S1 Cyclohexane oxidation with H_2O_2 in acetonitrile catalyzed by various osmium complexes and certain enzymes.

Entry	Catalyst	Concentration (M)	Time (h)	TON	Initial TON per 1 h (h^{-1})	Initial TON per 1 min (min^{-1})	Ref.
1	**1**	1×10^{-7}	24	200,200	16,200	270	this work
2	$Os_3(CO)_{12}$ [a]	5×10^{-6}	13	60,000	24,000	400	3g,h
3	Cp^*_2Os [b]	1×10^{-6}	24	51,000	6,000	100	3j
4	Cytochrome P450BM3 PFC9					110	9
5	Alkane ω-hydroxylase (AlkB) [c]					210	9
6	Soluble methane monooxygenase [d]					222	9

[a] Cyclooctane was used instead of cyclohexane.
[b] Decamethylosmocene, Cp* is pentamethylcyclopentadienyl.
[c] *n*-Octane was used instead of cyclohexane.
[d] Methane was used instead of cyclohexane.

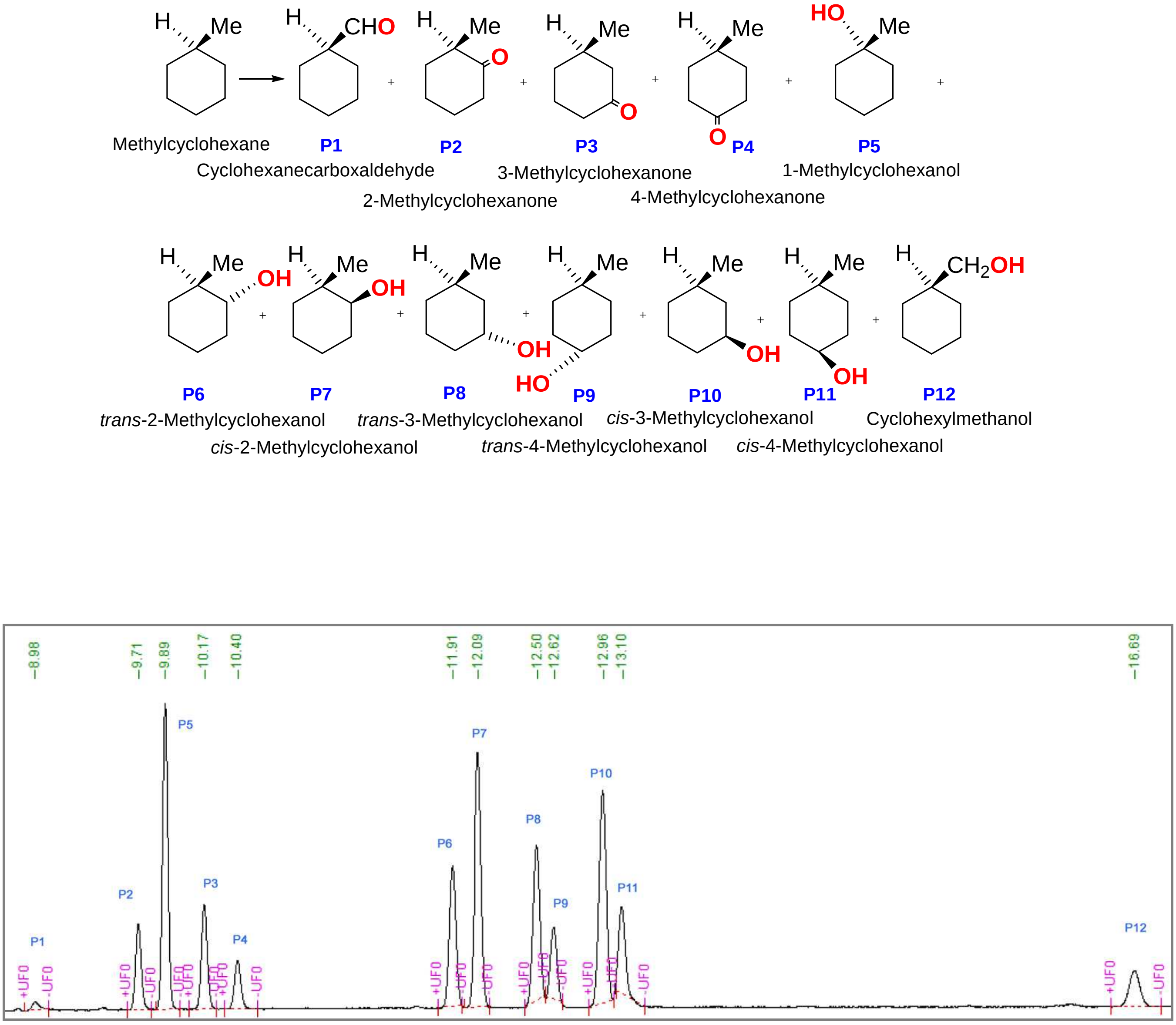

Figure S11. Products obtained in the methylcyclohexane oxidation (top) and chromatogram of the reaction mixture of the oxidation with the **1**/H_2O_2/py system (bottom). Concentrations (M) of products (after 1 h)**:** **P1** (0.00007), **P2** (0.00052), **P3** (0.00065), **P4** (0.00032), **P5** (0.0018), **P6** (0.0011), **P7** (0.0018), **P8** (0.0011), **P9** (0.0005), **P10** (0.0016), **P11** (0.0008), **P12** (0.0004). The selectivity parameter based on concentrations of alcohols (after reduction of the reaction mixture with PPh_3) is 1º:2º:3º = 1:5.2:13.8.

Appendix. Products of the cyclohexane over-oxidation with the $H_2{}^{16}O_2/{}^{18}O_2$ system

Usually, the isomers of cyclohexanediols and hydroxycyclohexanones are the most abundant by-products in the oxidation of cyclohexane by hydrogen peroxide as shown by equation (14).

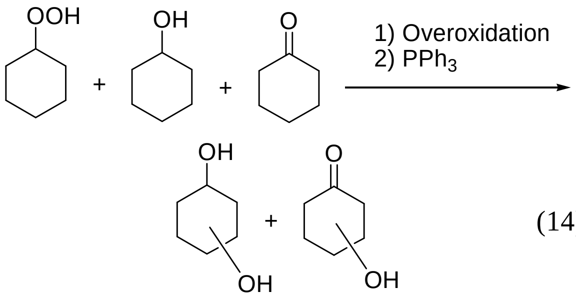

(14)

The analysis of chromatographic patterns (Figure S12) revealed five main byproducts. Their peaks become noticeable starting from the 0.06 M concentration of the main products (cyclohexanol and cyclohexanone). This corresponds to 13% yield based on the cyclohexane. The identification of the oxidation byproducts was made using the chromatograms of reaction mixtures obtained under proper conditions. With the cyclohexyl hydroperoxide (*cyclo*-$C_6H_{11}OOH$) as the main reaction product one may expect the formation of isomeric cyclohexane dihydroperoxides, *cyclo*-$C_6H_{10}(OOH)_2$, as the main overoxidation products which produce 1,2-, 1,3-, and 1,4-cyclohexanediols upon reduction with PPh_3.

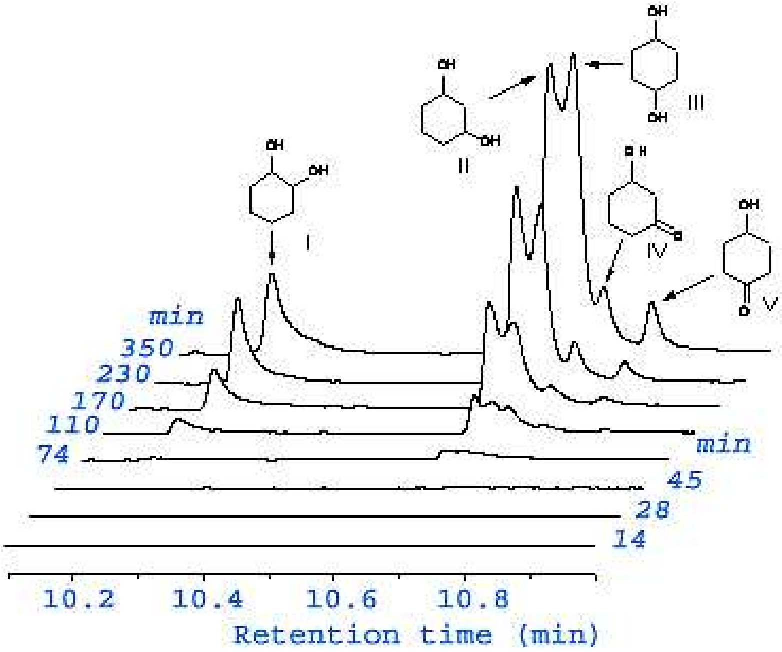

Fig. S12. The oxidation of cyclohexane by the **1**–py–H_2O_2 system in an ${}^{18}O_2$ the atmosphere. Chromatograms of the reaction samples taken after specific time intervals and reduced with PPh_3 show the accumulation of overoxidation products. The full mass-spectra of the products **I**–**V** are presented in Figure S13a-e).

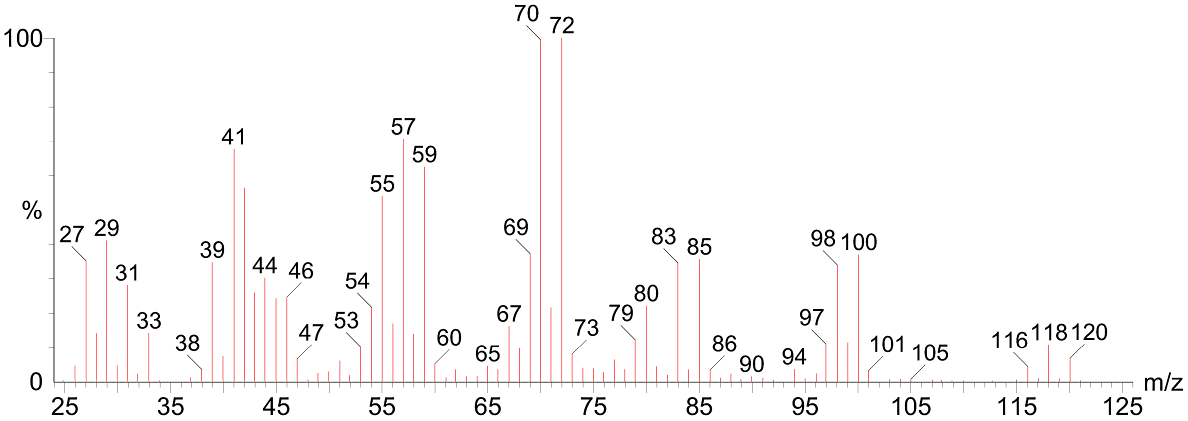

Figure S13a. Electron impact mass spectra of a mixture of unlabeled and ^{18}O-labeled 1,2-cyclohexanediols.

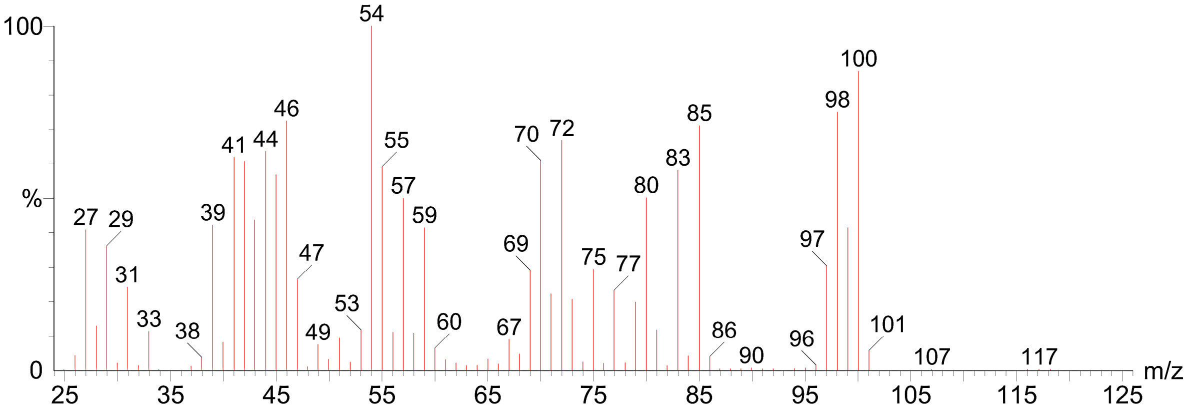

Figure S13b. Electron impact mass spectra of a mixture of unlabeled and ^{18}O-labeled 1,3-cyclohexanediols.

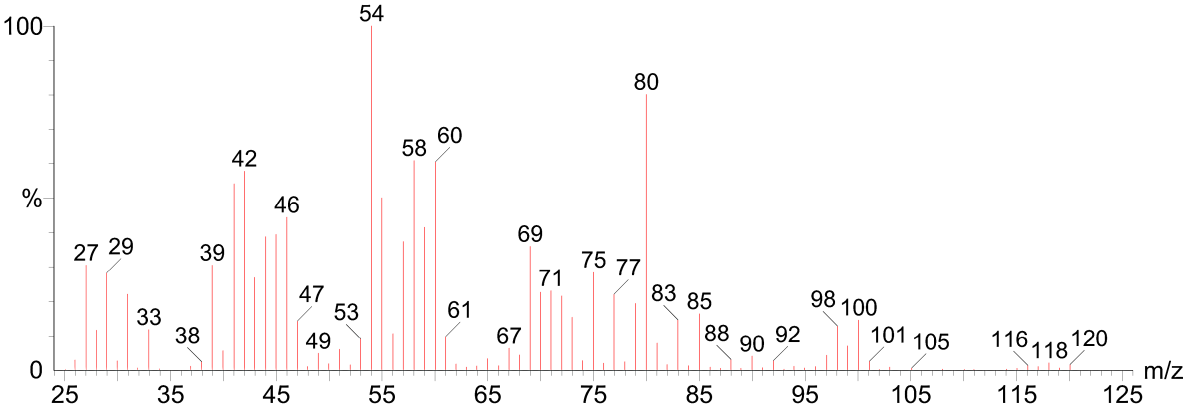

Figure S13c. Electron impact mass spectra of a mixture of unlabeled and ^{18}O-labeled 1,4-cyclohexanediols.

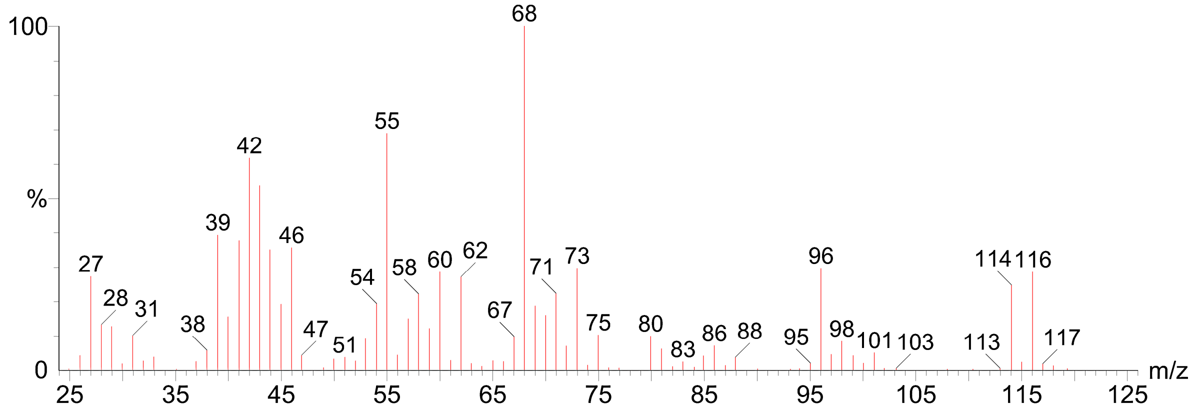

Figure S13d. Electron impact mass spectra of a mixture of unlabeled and ^{18}O-labeled 3-hydroxycyclohexanones.

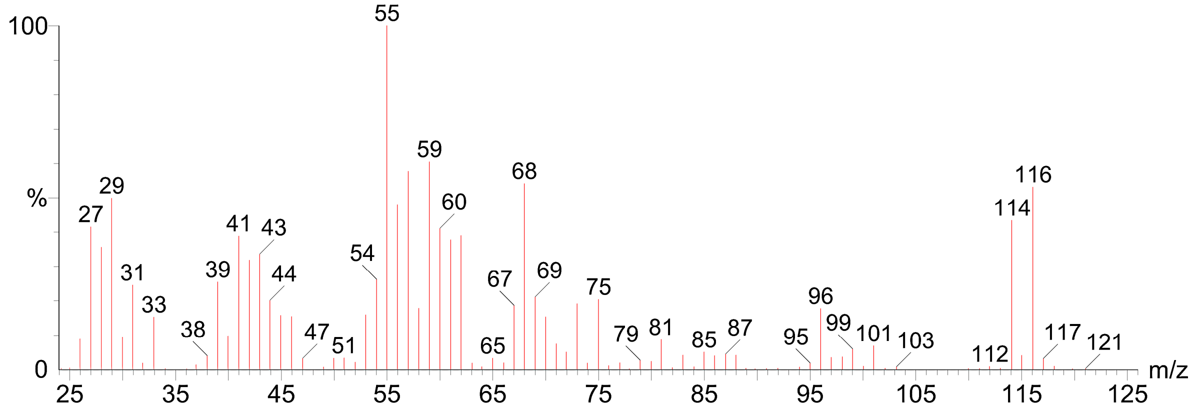

Figure S13e. Electron impact mass spectra of a mixture of unlabeled and ^{18}O-labeled 4-hydroxycyclohexanones.

The molecular ion peaks in the spectra of 1,2- and 1,4-cyclohexanediols are strong enough to estimate the isotopic distribution of labeled oxygen within the hydroxyl groups (Figure S14). In contrast, the molecular ion of 1,3-cyclohexanediol is much less stable and appears with only 0.2% intensity (Figure S13b). These results are in agreement with the reported mass-spectra of unlabeled 1,3-cyclohexanediol. [14a] Such a low intensity has not allowed us to correctly evaluate the intensity ratio of peaks 114 : 116 : 118 (attributed to unlabeled, single-labeled and double-labeled diols, respectively). To the best of our knowledge, the electron-impact mass spectra of isomeric 1,2-cyclohexanediols are the only ones studied in detail among all cyclohexanediols and therefore, unfortunately, the lack of data does not allow us to estimate the ^{18}O distribution mode in 1,3-cyclohexanediol. However, we assume that it is close to the distribution found for 1,2- and 1,4-diols.

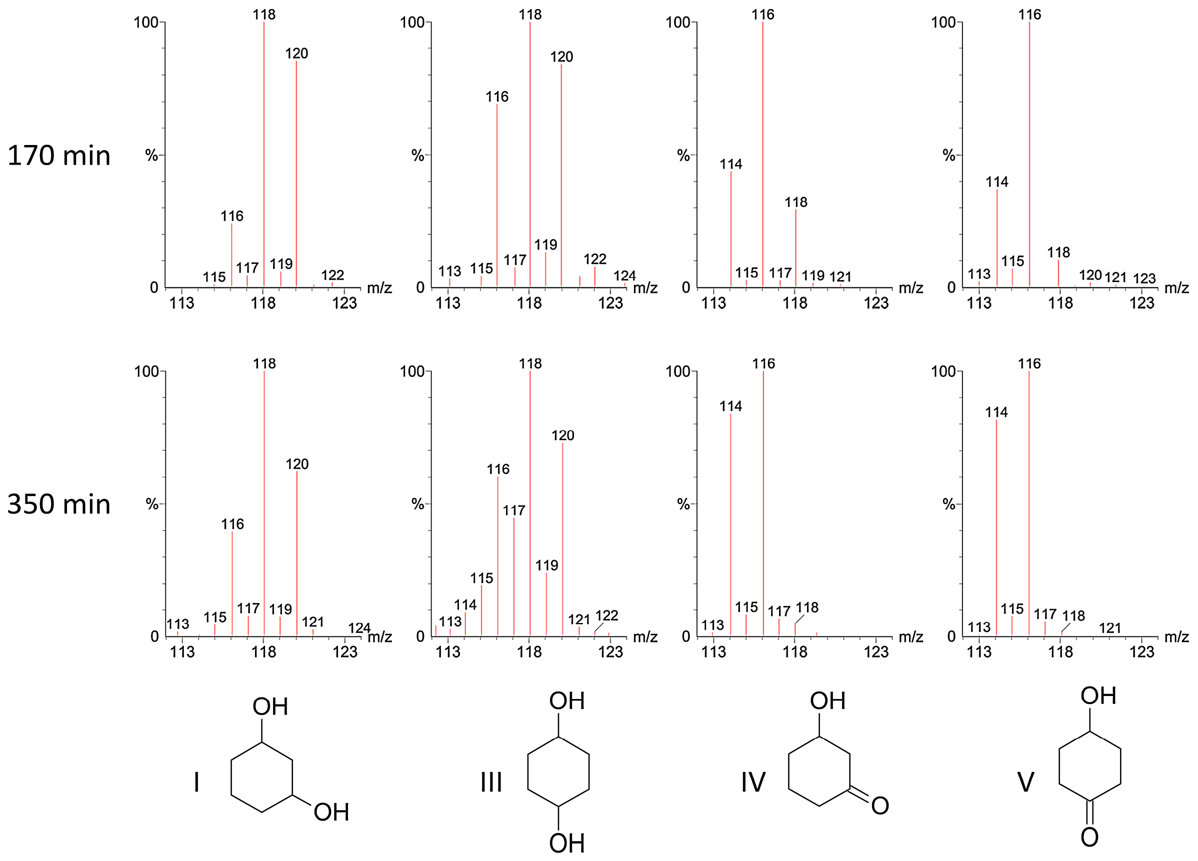

Fig. S14. Selected electron impact mass spectra (molecular ion peaks) of the overoxidation products.

Taking into account our observation that the major oxidation mechanism results in ca. 60 % of ^{18}O incorporation one may expect the following distribution of labeled diols: 16 : 48 : 36 % for ^{16}O–^{16}O, ^{16}O–^{18}O and ^{18}O–^{18}O combinations, respectively. The respective ratios for overoxidation products **I** and **III** (Figure S12) measured after 370 min reaction time (20 : 50 : 30 and 28 : 39 : 33 for **I** and **III**, respectively) are in a good agreement with the expected distribution. The mass spectra of the sample taken at 170 min show increased amounts of a doubly-labeled diols (Figure S14) as well as hydroxyketones. These results are in agreement with the general dependence of the ^{18}O incorporation into the cyclohexanol and cyclohexanone (Figure 11).

The molecular ion peaks of 1,3- and 1,4-hydroxycyclohexanones in the sample taken at 350 min clearly demonstrate that the doubly-labeled species are almost absent, with ca. 55% incorporation of ^{18}O into the single-labeled ones (Figure S14). This could be understood if we consider the reaction scheme where ketones are formed via a minor pathway which does not involve the reaction with O_2 (see the main text). In such case, both ketonization of cyclohexyl hydroperoxide Cy–$^{18}O^{18}OH$ and hydroxylation of ketone *cyclo*-C_6H_{10}=^{16}O should afford hydroxycyclohexanone having only labeled hydroxy group. The peak of 1,4-hydroxycyclohexanone (product **V**) is well separated from other peaks in the chromatogram (Figure S12) and due to this its mass spectrum was used in order to determine if the labeled oxygen is located either in the ketone or alcohol group.

The mass spectra of 1,4-hydroxycyclohexanone (product **V**) obtained from the catalytic oxygenation of C_6H_{12} under $^{18}O_2$, C_6H_{12} under air and C_6D_{12} under air are shown in Figure S15.

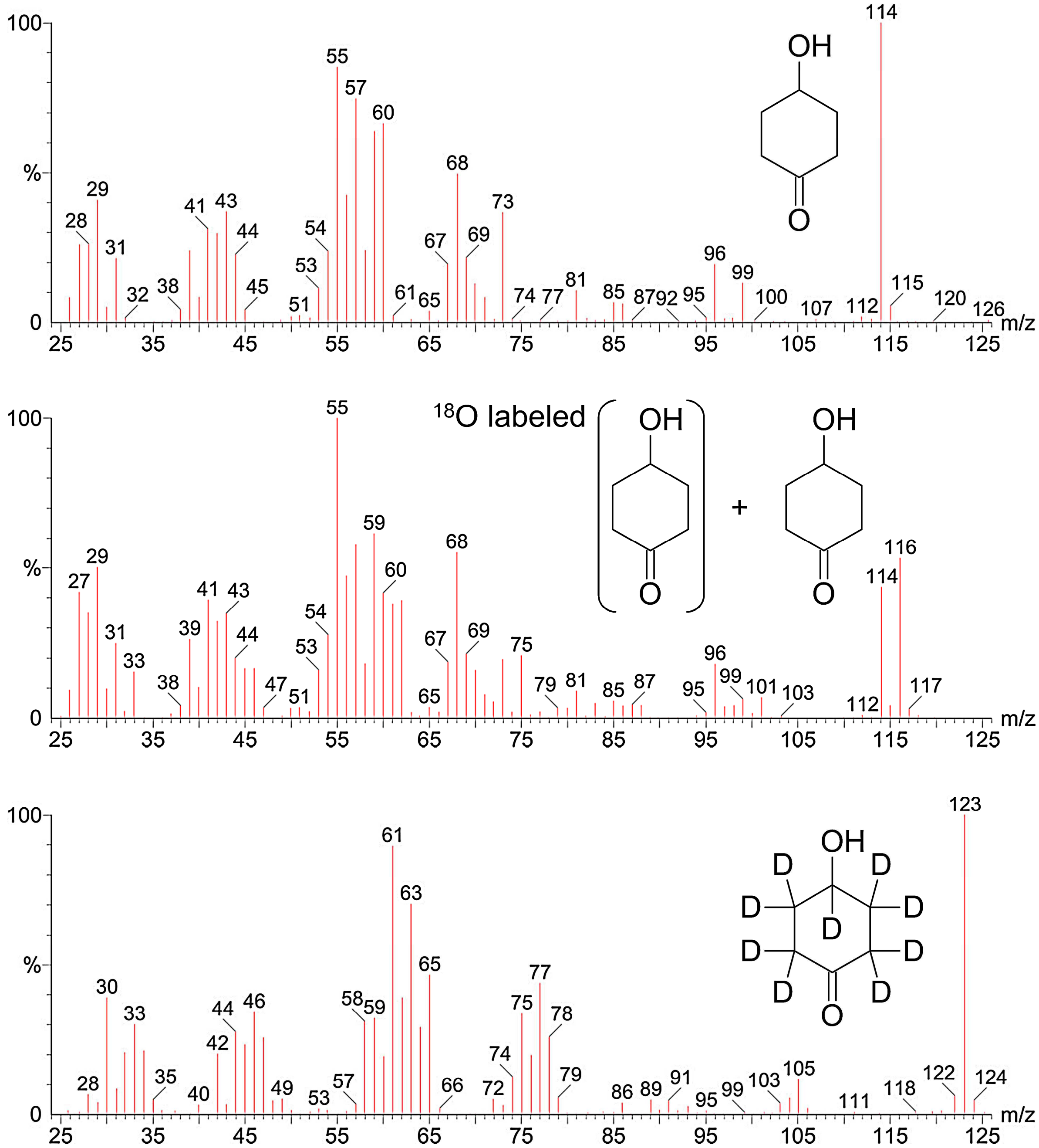

Figure S15. Electron impact mass spectra of pure 4-hydroxycyclohexanone (**V**, top), a mixture of unlabeled and labeled **V** (middle) and deuterated **V** (bottom).

It has long been known that compound **V** undergoes oxygen rearrangement on electron impact forming species *c* and *d* at 60 and 73 m/z, respectively (Scheme S1). [14b] Although the mechanism of such rearrangement was proved by numerous experimental data these species do not help us to identify the location of the labeled oxygen which can be present both in ketone and alcohol groups. Cyclohexanone itself is known to eliminate the propyl fragment through two α-cleavages producing species *a* at 55 m/z. [14c-e] One may expect the existence of such mechanism in the decomposition of hydroxycyclohexanones under electron impact. However, the relatively low intensity of the corresponding 58 m/z peak in the spectrum of deuterated product **V** indicates that the proposed attribution is doubtful for the case of compound **V**.

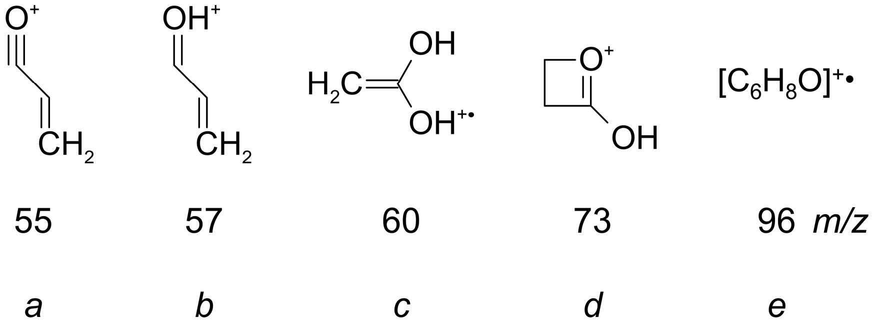

Scheme S1. Possible ions which are formed from 4-hydroxycyclohexanone upon electron impact.

The peak at 57 m/z was definitely assigned to the species *b* in the spectra of cyclohexanol.[14f,g] Further, it was shown that the higher homolog of species *b* is easily formed from 4-methyl-4-hydroxycyclohexanone. [14b] Considering the presence of a peak at 61 m/z in the spectrum of deuterated product **V** (species *b* containing three D atoms) with an intensity equal to that for non-deuterated **V** we assume that the lowering of the peak 61 m/z from 92 to 62 % could be attributed to 57 → 59 m/z shift due to ^{18}O labeling of the hydroxy group (here and further the percentage intensities will be given relative to the molecular ion peak intensity). However, the intensities of the respective 59 m/z peak are almost equal for both labeled and unlabeled compound **V** (Figure S15). This effect can be explained by the presence of some unidentified species at 59 (63 %) for normal and 61 (39 %) m/z for labeled compound **V**. From these data the estimated intensity of 59 m/z peak in the spectrum of the labeled product **V** (labeled species *d* plus unlabeled *e*) is ca. 61 %. This value is very close to the observed intensity of 63 % (Figure S15). These data show that the over-oxidation product **V** should be labeled preferably into the hydroxyl group.

Further, it is known that cyclohexanol shows an intensive peak of species $[C_6H_{10}]^{+\cdot}$ at 82 m/z which is formed by elimination of HOH from the molecular radical cation. [14f,g] Therefore, the peaks at 96 and 104 m/z (for "light" and deuterated compounds, respectively) in the spectra of product **V** can be attributed to fragment *e* $[M–HOH]^{+\cdot}$ (Scheme S1) in which the oxygen atom is preferably originated from the ketone group. Due to the absence of ^{18}O atoms the spectra of unlabeled compound **V** do not show any noticeable peaks at *e* + 2 *m/z*. In the case of labeled product **V** the low intensity peak at 98 m/z is observed which can be attributed to ^{18}O-containing particle *e*. From the relative intensities of the peaks at 96 and 96 m/z the isotope labeling ratio of ketone and hydroxyl groups can be estimated to be ca. 30 : 70. However, taking onto account the complexity of the HOH elimination process which can proceed *via* different mechanisms [14h] we cannot exclude the elimination of the oxygen atom from the ketone group during the formation of species $[M\text{–}HOH]^{+\cdot}$. Therefore, the real portion of the ^{18}O-ketone in the labeled product **V** could be much lower than 30%. Such an assumption is confirmed by the evaluation of the 57–61 m/z peaks intensities described above.

Interestingly, noticeable amounts of hydroxyacetonitrile HO–CH$_2$–CN were detected by the chromatograms of benzene oxidation samples (Figure S16). This byproduct has never been detected in the oxidation of saturated hydrocarbons using the technique described here although the interaction of hydroxyl radical with CH$_3$CN is always taken into account when describing the reaction mechanisms (see above, Section 3.5). We found that according to the mass-spectral data (Figure S17) hydroxyacetonitrile contains ca. 55% of the ^{18}O isotope.

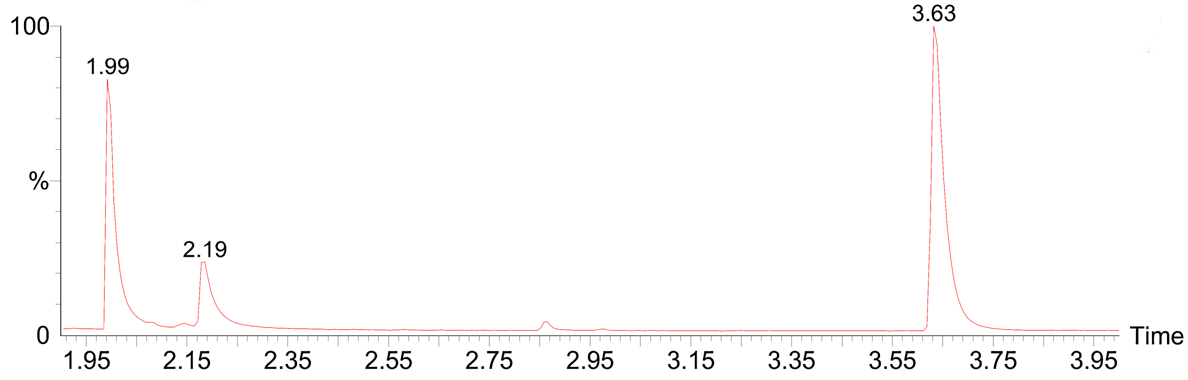

Figure S16. Chromatogram of the reaction mixture at 4.5 h time (taken after PPh$_3$ addition). Three largest peaks correspond to pyridine, ^{18}O labeled hydroxyacetonitrile and unlabeled phenol, respectively.

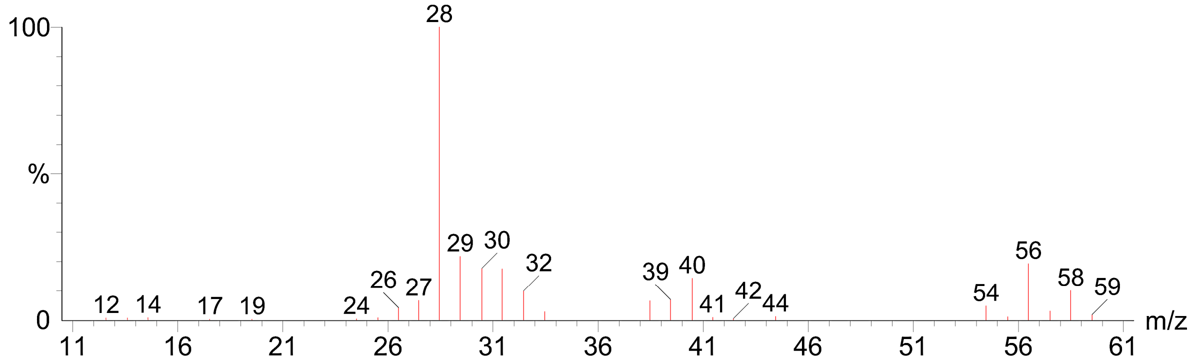

Figure S17. Electron impact mass spectrum of a mixture of unlabeled and ^{18}O-labeled hydroxyacetonitrile.

Additional references to Appendix

(14) (a) US National Institute of Standards and Technology (NIST) Mass Spectral Library, ver. 2.0f, build Apr. 1, 2009. (b) Green, M. M.; Djerassi, C. *J. Am. Chem. Soc.* **1967**, *89*, 5190–5198. (c) Gross, J. H. *Mass Spectrometry, A Textbook*; 2nd edition, Springer-Verlag: Berlin/Heidelberg, 2011. (d) Williams, D. H.; Budzikiewicz, H.; Pelah, Z.; Djerassi, C. *Monatsh. Chem.* **1964,** *95*, 166–177. (e) Seibl, J.; Gäumann, T. *Helv. Chim. Acta* **1963,** *46*, 2857–2872. (f) Holmes, J. L.; McGillivray, D.; Rye, R. T. B. *Org. Mass. Spectr*. **1973**, **7**, 347–356. (g) Shapiro, R. H.; Levine, S. P. *Org. Mass. Spectr*. **1971**, *5*, 383–388. (h) Ward, R. S.; Williams, D. H. *J. Org. Chem.* **1969**, *34*, 3373–3377.